# Structure of Long Island's Carolina Bays and Their Potential Relationship to the Proposed Younger Dryas Impact Event

Sean Tvelia

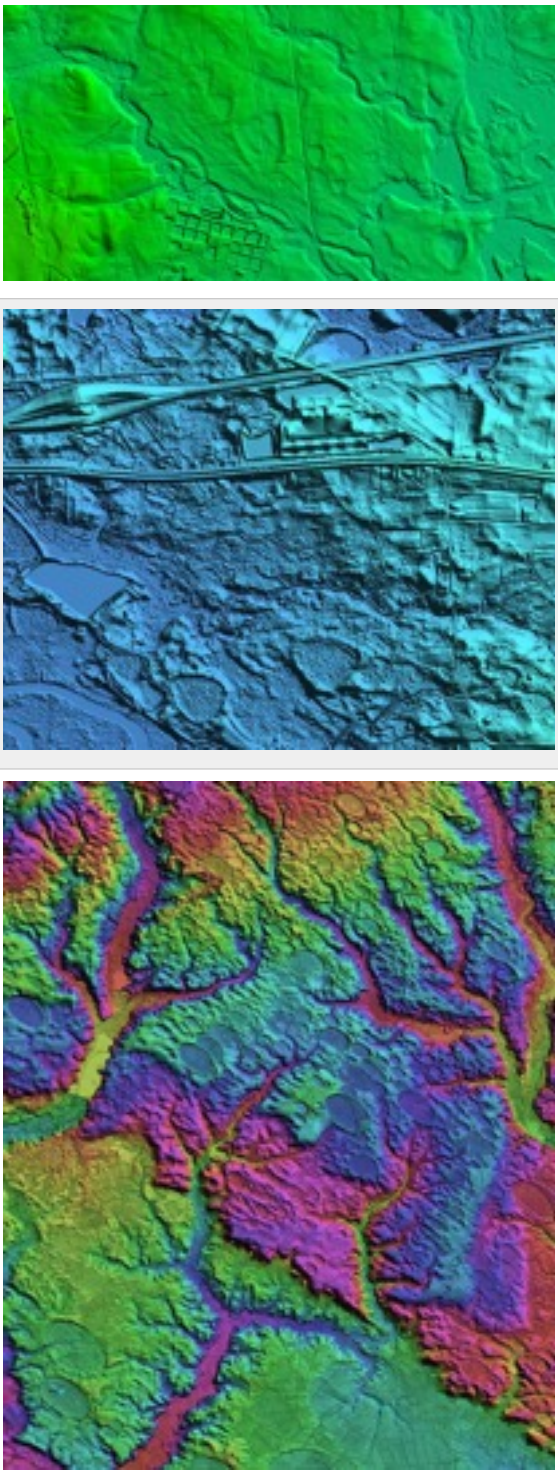

Figure 1. Comparison of Carolina Bays from Long Island, NY (top); Deleware Memorial Bridge, NJ (middle); and Bennetsville, SC (bottom) showing change in shape from oval/ elliptical in south to bell shape in north.

Recent high-resolution lidar and orthoimages of Long island have revealed numerous low relief depressions across portions of Suffolk County that are inconsistent with the more typical glacial features such as kettle holes and thermal karst depressions found within the region. Unlike kettles these features rarely exceed 4ft of relief and have similar bell-shaped appearance and rims that extend around the entirety of the depression, with parallel long axis trending in a south-easterly direction. Due primarily to their alignment, consistency in shape and similarity to other known features these depressions have been investigated as potential Carolina bay-like structures. Like Carolina bays the process by which these features form has yet to be conclusively determined and may be the result of thermokarst processes or impact cratering related to the controversial Younger Dryas impact event first put forth by Firestone *et. al* (Firestone 2007).

Amongst the evidence first put forth by Firestone in support of an impact related hypothesis is "discrete layer with varying peak abundances of (i) magnetic grains with iridium, (ii)magnetic microspherules,(iii)charcoal, (iv)soot,(v)carbonspherules,(vi)glass-like carbon containing nanodiamonds, and (vii)fullerenes with ET helium (Firestone, 2007)" that has been identified at numerous Younger Dryas boundary sites. Since it was first published this hypothesis has been the subject of much debate with numerous studies, such as those by van Hoesel (2012) & (2014) which point to terrestrial explanations for magnetic spherules, Rodriguez (2012) which provides eolian processes for the creation of the rims of some Carolina bays, Scott (2010) who provides alternative routes of formation for carbon spherules, and Pinter (2014) who summed up the critiques of the hypothesis and declared the debate over. A major point made by many critics of the Firestone hypothesis is the

inability of some authors to reproduce results first shown by Firestone (2007). However these critiques seem to overlook studies such as la Compte (2012) that were able to reproduce similar results and determined that the inability to reproduce results were due to the failure to follow the prescribed protocol outlined by Firestone (2007).

This current study looks to advance our understanding of the processes associated with the formation of Long Island's Carolina bay-like structures and their potential relationship to events surrounding the onset of Younger Dryas through geophysical and stratigraphical means.

**Carolina bays**

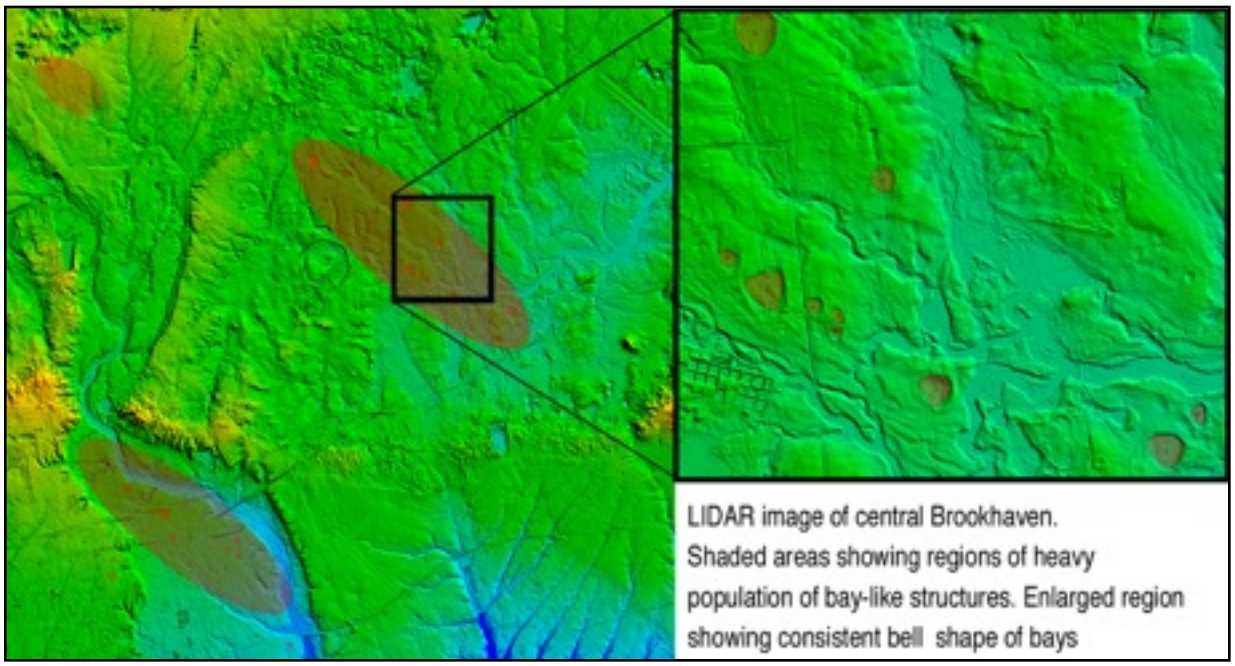


Figure 3: DEM of Central Brookhaven, NY. Shaded ovals showing regions of abundant bay-like structures. Individual bays shaded in red.

Carolina bays have been identified along the East coast from northern Florida to New Jersey and are characterized by nine distinctive features as described by the South Carolina Department of Natural Resources(SC Dept. of Natural Resources 1999):

1. elliptical or oval shape
2. northwest-southeast orientation
3. parallel axes
4. raised sand rims
5. depressed interior surfaces
6. difference between interior and surrounding soils
7. relatively shallow depths
8. flat sandy bottoms beneath interior fill

Over 74 bay-like structures have been identified across eastern Suffolk County (Gill, nd). These structures often occur in linear tracts with similar bearings as the major axis of the individual structures. Like similar structures identified in New Jersey, Longs Islands bays consist of bell-shaped depressions. Although South Carolina's bays, as described above, are characterized by an oval to elliptical shape, the shape of Carolina bays range from oval/elliptical in more southern regions to bell shape depressions in more northern regions as shown in figure 1 (Gill, nd).

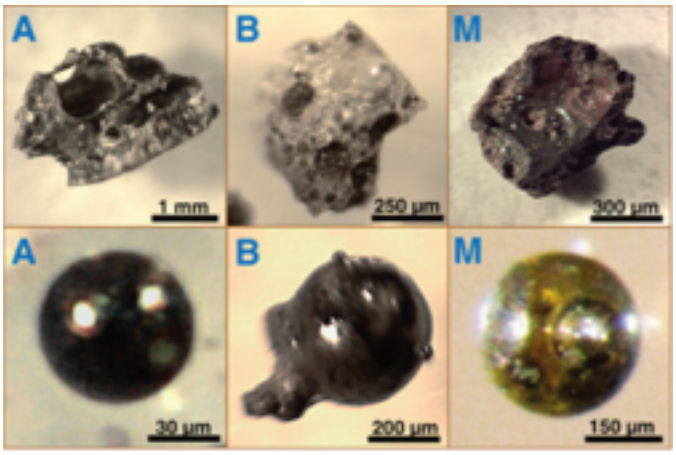


Figure 2. Light photomicrograph of microspherules and SLO from Syria, South Carolina, and Pennsylvania. adapted from Van Hoesel (Van Hoesel 2004)

The formation of Carolina Bays is still not fully understood and research has provided numerous mechanisms including the charging of ground water, thermal karst activity, prograding lake shores with dune accretion, and impact cratering(Rodriguez, 2012). Debate over the most controversial mechanism, impact cratering, was recently reignited by Firestone (Firestone, 2007) when it was proposed that an extraterrestrial impact occurred 12,900 years ago over the Laurentide Ice Sheet and eventually lead to Younger Dryas cooling event, extinction of the North American megafauna, and the decline of clovis culture.

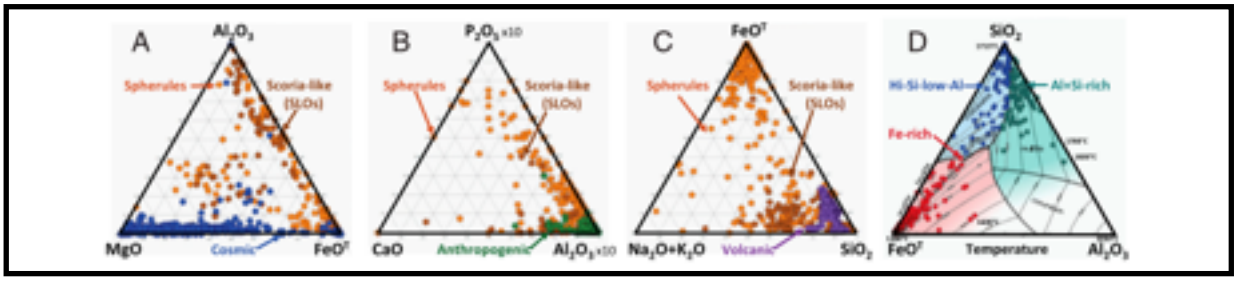


Figure 3. Ternary diagrams comparing molar oxide wt from younger dryas SLO's (dark orange) to (A) cosmic material, anthropogenic material and (C) volcanic material. Adapted from Bunch 2012.

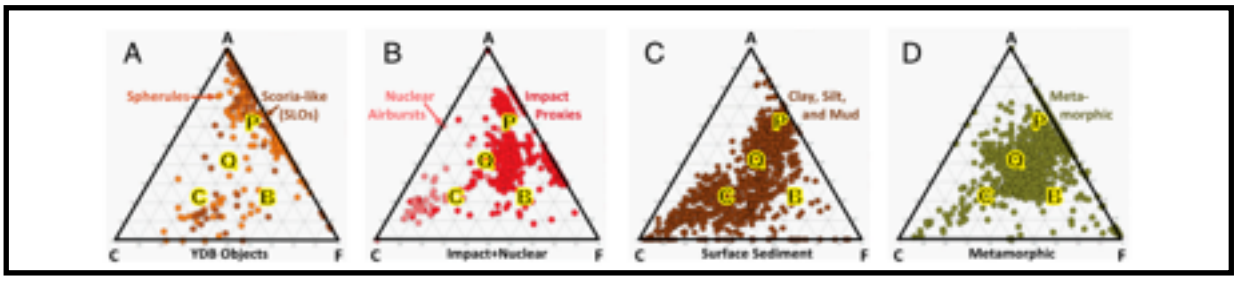


Figure 4. Ternary diagrams comparing SLO to specific metamorphic rock types; P-pelitic, Q-quartzofeldspathic, B- Basic, and C-calcareous. Adapted from Bunch 2012.

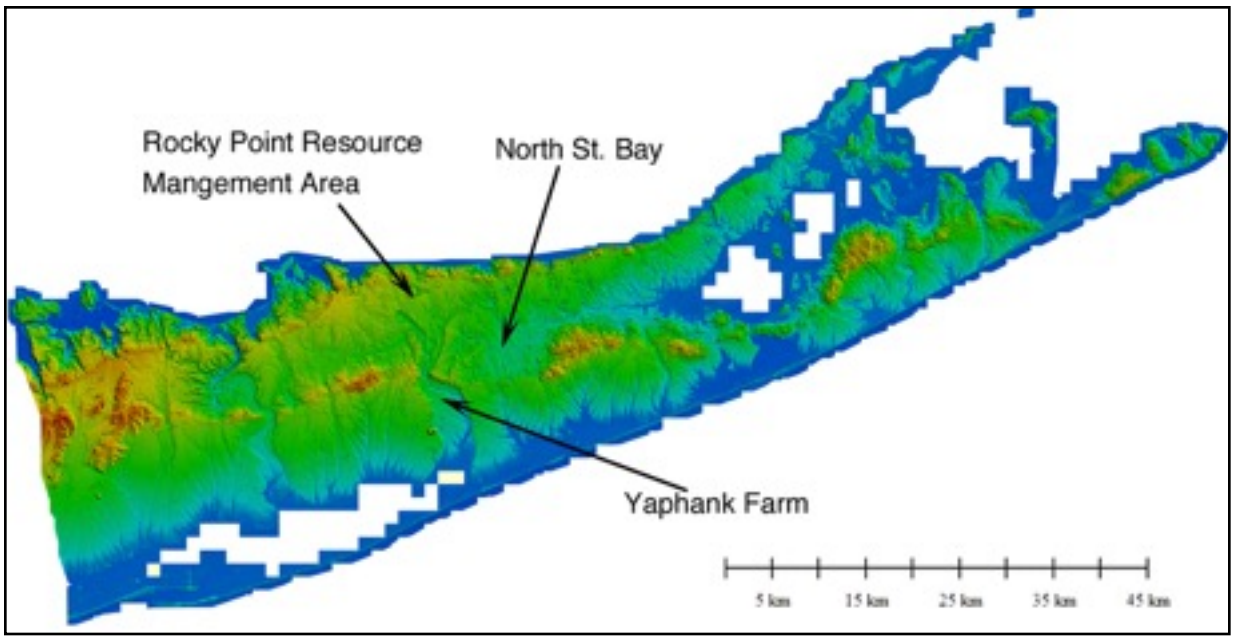


Figure 5. DEM of Long Island, NY showing locations of current and future study sites.

As evidence for this impact Firestone cites peak abundances of various impact markers, including magnetic microspherules, magnetic grains with increased iridium, charcoal, carbon spherules, nano diamonds, and fullerenes containing extraterrestrial helium (Firestone, 2007) in discreet layers at the Allerod-Younger Dryas (AYD) boundary. Firestone further notes that the boundary extended throughout “at least 15 Carolina bays” (Firestone 2007). However, as noted by Van Hoesel (Van Hoesel 2014), of the evidence put forth in favor of the impact hypothesis only increased abundance of iridium is considered a diagnostic marker of extraterrestrial impact and, although numerous studies have been able to confirm many of the results cited by Firestone, work on at least two AYD boundary locations failed to reproduce similar findings.

Since Firestone’s initial publication, researchers have also noted the presence of scoria-like objects (SLO’s) within the sediment at AYD boundary sites in Syria, South Carolina, and Pennsylvania that also contained microspherules and magnetic grains(Bunch, 2012). Assays by Bunch *et. al* show these sediments to be compositionally distinct from those produced within volcanic plumes with volcanic SLO’s enriched 2X in $Na_2O$ + $K_2O$ compared to those of the AYD boundary. Bunch also determined that AYD SLO’s are enriched in Fe 5.5X

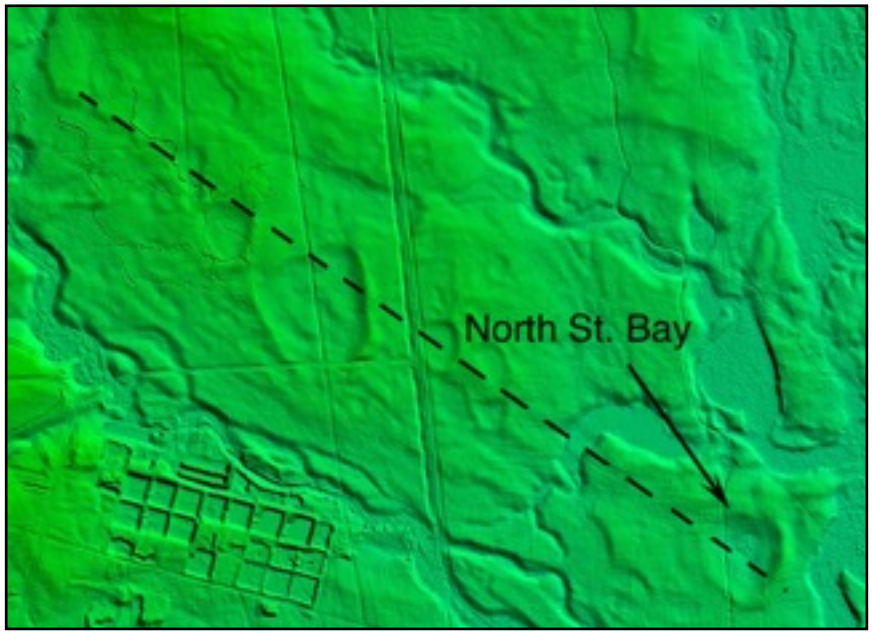


Figure 6. DEM of North St Bay showing linear pattern of bays and position of the North St Bay. Dotted path showing 120° bearing.

compared to known volcanic SLO, see figure 3 (Bunch, 2012). Bunch et. al further surmise that the presence of low-viscosity flow bands found in many SLO's suggest final temperatures greater than 2,200°C and as such could not be the result of terrestrial processes(Bunch, 2012).

**Study Sites**

To determine the processes that formed Long Island's bay-like structures, three sites have been targeted for study; these include the North Street bays, the Rocky Point Resource Management Area, and the Suffolk County Farm in Yaphank, NY. These sites, shown in figure 5, were chosen based on the degree to which depression morphology matches that of previously identified Carolina bays, the prevalence of bays within the region, and the ease of access to the site.

The North St. Bay is located at the southern end of a linear tract of depressions with a bearing of roughly 120°, see figure 6. Individual depressions within the tract have bell-shaped appearances and an all-encompassing rim which often reaches maximum elevation along the south eastern wall of the features. Total relief of individual depressions ranges from slightly over 1m to 3.5m in the North St. Bay.

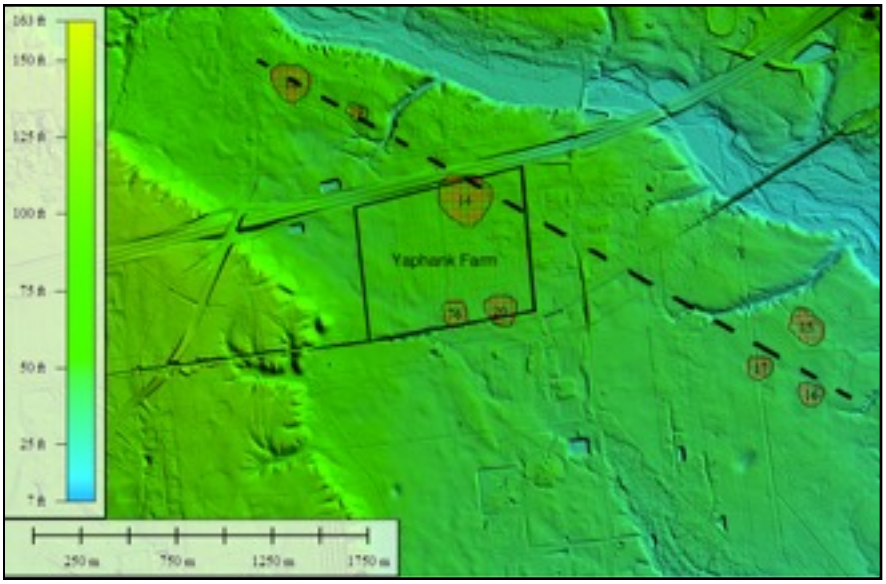


Figure 7. DEM of Carman's river meltwater valley showing location of Suffolk County (Yaphank) Farm and distribution of bay-like structures. Dotted path showing 120° bearing.

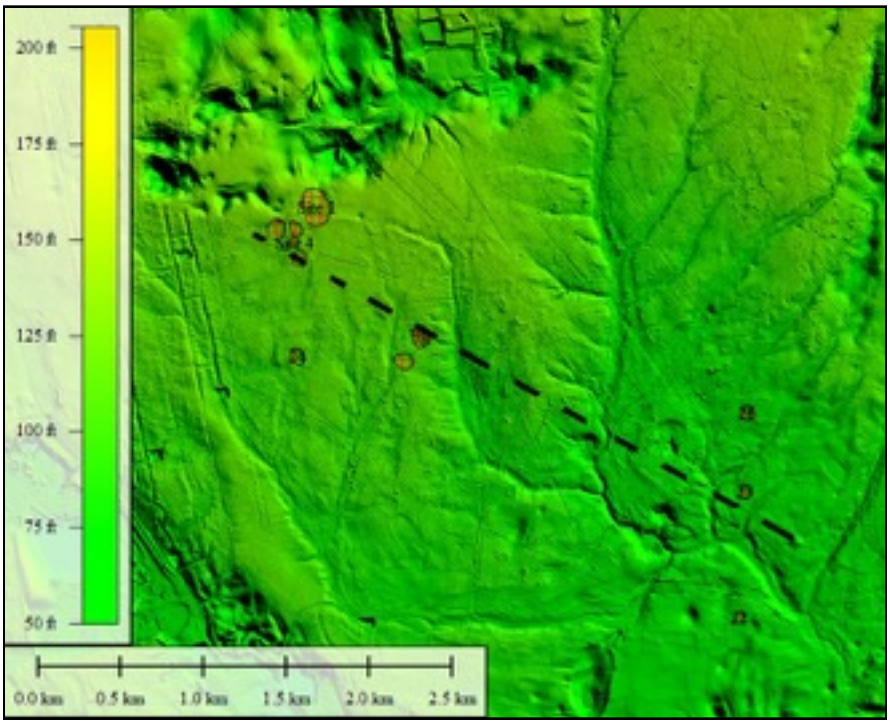


Figure 8. DEM of Rocky Point Resource Management Area showing locations of bay-like structures. Dotted path showing 120° bearing.

The Suffolk County Farm in Yaphank, NY, is located on the former flood plain of the Carman Rriver meltwater channel. At least three bay-like structures have been located within the fields

on the property and although located in active growing fields the raised rims of the bays are still distinguishable in LIDAR images. Like the North St. Bays, these structures seem to occur within a linear pattern, bearing of roughly 120°, within the meltwater valley.

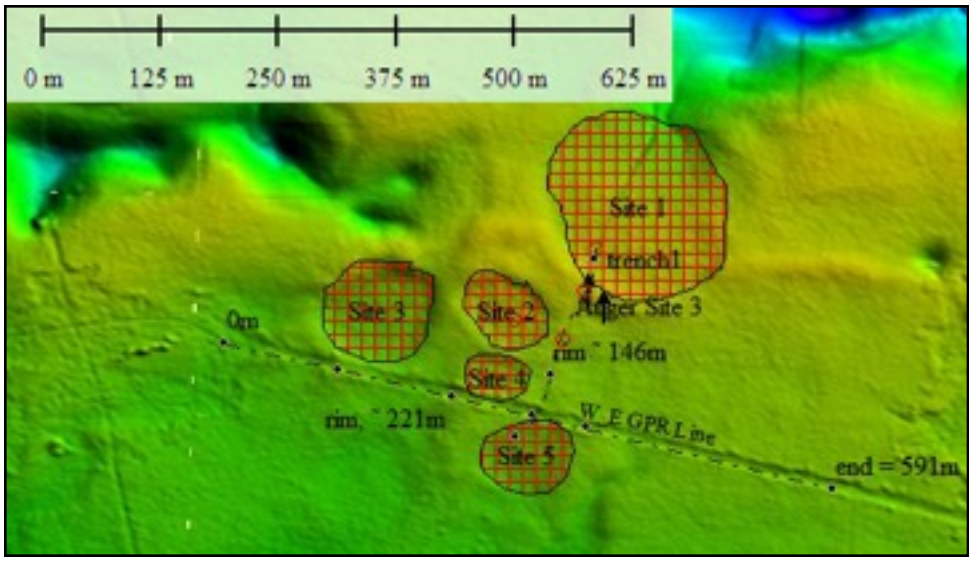


Figure 9. Site Plan showing multiple bay like structures, GPR tracks (dotted black lines), trench site (arrows), and auger sampling indicated by red circles.

The Rocky Point Resource Management Property is located north of the Carman River meltwater channel in an area of raised elevation that is most likely the result of deformation within an interlobate region of the laurentide icesheet. Like the North St and Suffolk County Farm sites, bay-like depressions within this region follow a similar linear tract of bearing 120°. Continuation along this bearing from the Rocky Point site also leads directly to the North St. Bay.

The consistent linear pattern and bearing as well as the shape of these bay like depressions is consistent with an impact cratering event potentially related to secondary impactors from the AYD boundary event. Furthermore, sediment and soil studies showing a pervasive capping of pebbly loess across most of these regions may also be the ejecta blanket from such an event.

**The Rocky Point Resource Management Area**

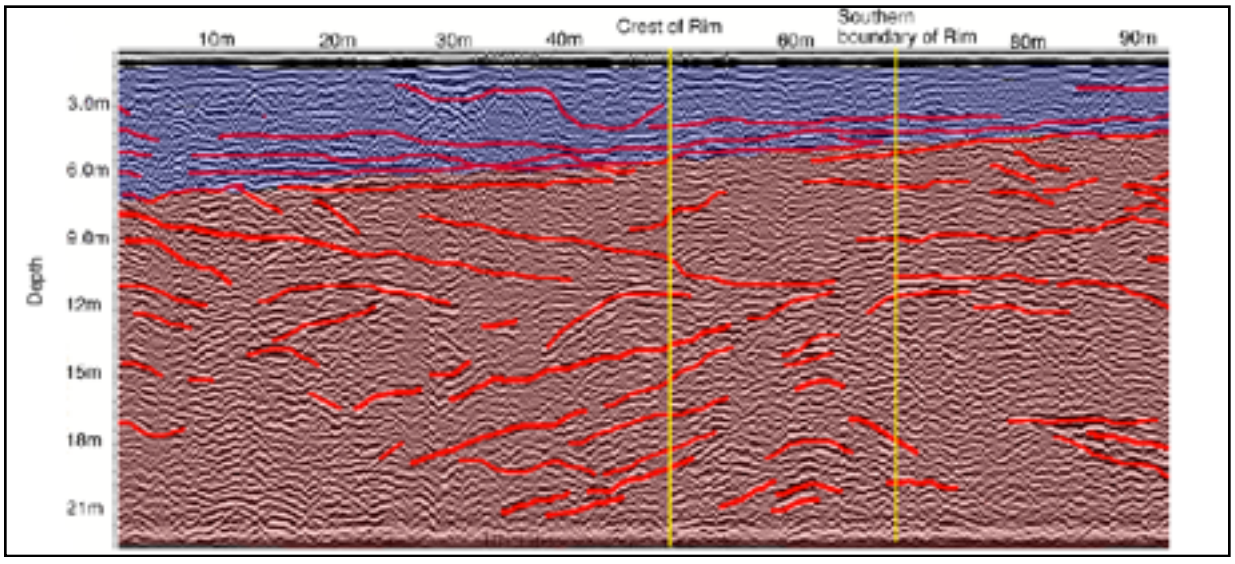


Figure 10. 200mHz Radargram showing first 90 meters of N-S GPR track. Vertical yellow line indicating the location of the rim along site 1.

This paper will focus on the initial results of stratigraphical and geophysical studies of the Rocky Point Resource Management Area. The site consists of numerous rimmed depressions in relatively close proximity, identified as Sites 1-5 in figure 9. An existing foot path runs north-northeasterly across the site transacting the largest depression, site 1, and along the eastern rim of another, site 2. Another previously existing path runs perpendicular to the north-south path and the two paths intersect along the north rim of the bay identified as site 5 in figure 9.

GPR studies were conducted along both the N-S and E-W paths using 200mHz RAMAC antennas and processed using GroundWave software. Radiograms of the N-S track reveal no distinctive features indicative of either impact or thermal karst activity but do reveal areas of highly deformed bedding occurring within the largest bay-like depression. As can be seen in figures 10 & 11 two distinct units are identifiable based on the orientations of beds; an upper unit that


Figure 12. Photograph of trench dug parallel to the N-S GPR line showing upper unit of unstratified pebble loess and lower pebble sand unit. Scale in English units.

extends the entire distance of the survey containing parallel bedding and an upper till layer between 1.2 and 1.8 meters of depth which is identified by numerous hyperbolic reflectors; and a lower unit consisting of highly deformed beds in the north and more parallel beds towards the south of the track.

Unlike the N-S track, GPR along the W-E track reveals little to no deformation and although a glacial till boundary is observable at similar depth as in the N-S track, two till boundaries appear to be present along the rim of the site 2 depression, see W-E GPR track in appendix.

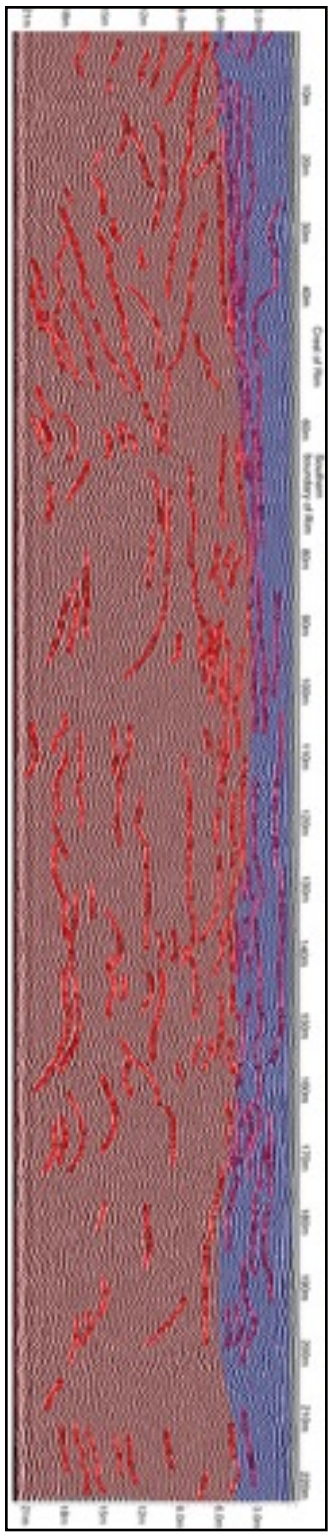

Figure 11. Radargram of N-S GPR track. Blue and red shading showing identified units and red lines indicating stratigraphy and reflectors.

In order to truth the GPR a small trench was dug parallel to the N-S GPR track, identified by the arrow and labelled trench 1 in figure 9. As can be seen in figure 12 much of the rim consisted of unstratified pebbly loess which extended to a depth of roughly 1 meter and was overlying loose white pebbly sands. The boundary between these two layers corresponds to a brightly reflecting boundary near 1.2 meters depth visible on the N-S GPR track.

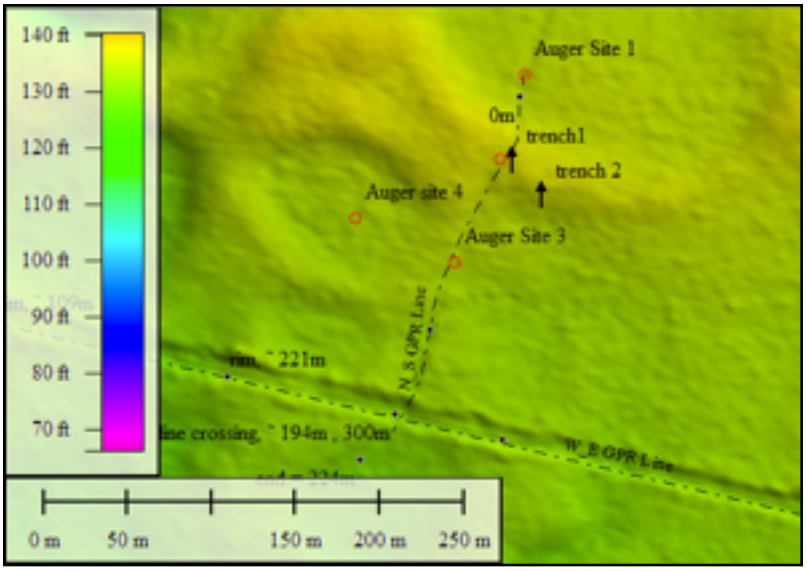


Figure 13: Location of Auger sites in relation to N-S and W-E GPR lines

Auger sampling was conducted at three different locations along the N-S GPR track: the zero mark, the crest of the northern rim, and along the the rim of the depression labelled site 2 in figure 9. A fourth auger sample was conducted in the center of the depression labelled site 2 in figure 13. Sediment samples, representing distinct units based on color and texture were collected from the bore hole located along the northern rim. These samples were air dried, weighed, and sieved.

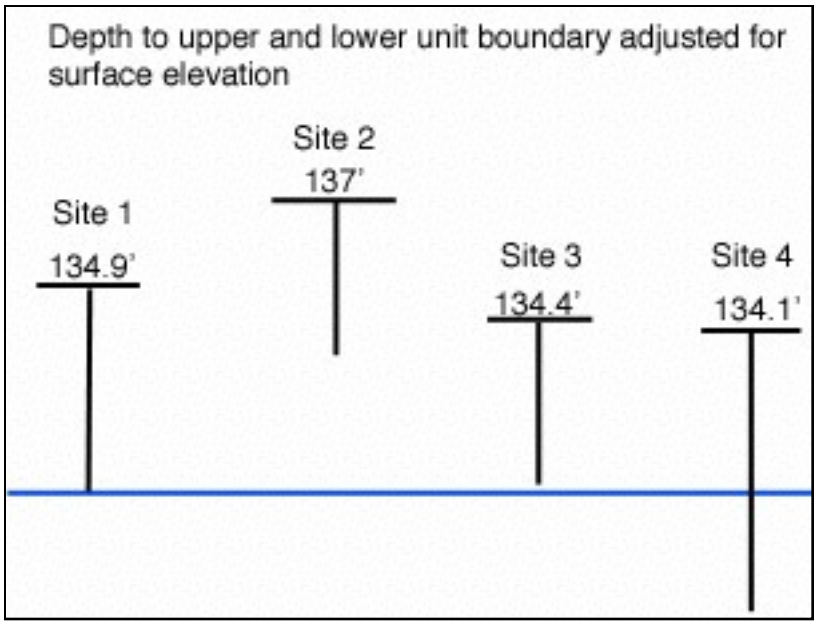


Figure 14: Graphical representation of depth to lower unit boundary adjusted for surface elevation. Blue line represent equal elevation of 130' above sea-level.

At each site the upper unit shown in the GPR consisted of most orange silty sands with increasing abundance of pebbles with depth. At it's greatest depth this unit transitioned from orange to gray and was underlain by extremely loose dry white poorly sorted sands with medium gravel which was difficult to bring up with the 3" auger.

As can be seen in figure 14 the boundary between the upper and lower units, represented by the base of the vertical bar, appears to correlate with surface topography from site 1 to site 3—moving across the rim of the large northern bay.

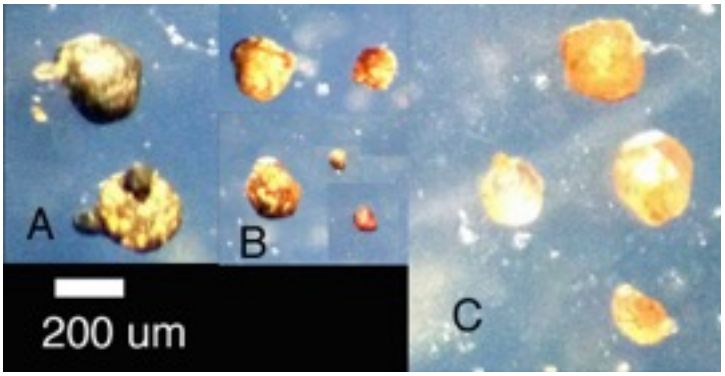


Figure 16: Photomicrograph of a representative sample of microspherules recovered from auger site 4. A, black glassy spherules; B red glassy spherules; C colorless spherules

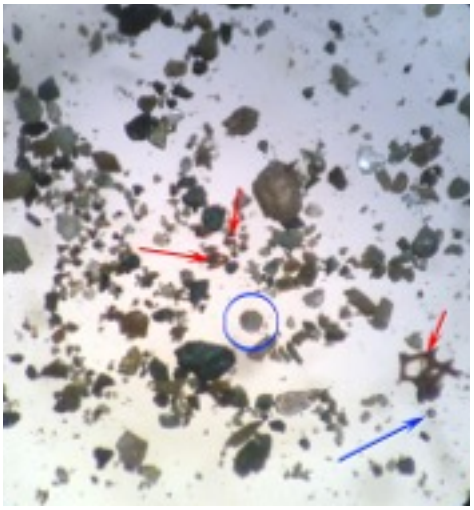

Figure 15: Photomicrograph of bulk magnetic grains collected from auger site 4. Blue arrows indicating microspherules; red arrow indicating scoria like objects.

The boundary between the upper and lower units represents the lowest extent of augering due to the ability to bring the loose sediments of the lower unit to the surface within the auger. Nevertheless it is believed based on the presence of numerous hyperbolic reflectors within the N-S GPR line near the same depth that this boundary may be the upper surface of a glacial till unit. Representative samples of distinctive units within each auger site were bagged and logged for analysis.

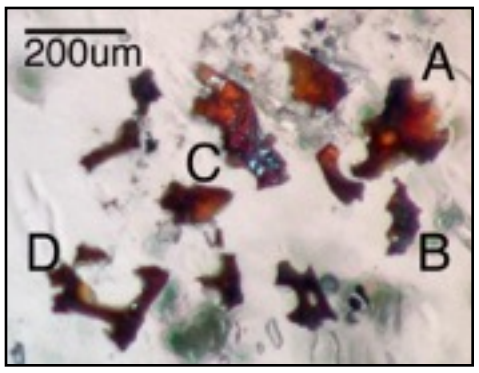


Figure 17: Photomicrogaph of scoria-like objects. Labels match that of corresponding spectra SLO1-B and SLO1-D.

**Sample Analysis**

The bagged sample (128g) of the pebbly sand unit at the base of the bore holes was air dried and sampled for the presence of magnetic grains using a 42N neodymium magnet. The magnet was wrapped in a 1qt ziplock bag and placed within the sample bag. The sample was then gently mixed for one minute. The magnet was then removed and grains were collected in a pyrex petri dish for analysis under stereo microscope. As can be seen in figure 15, bulk samples of magnetic grains consist of angular to sub angular grains of magnetite, quartz, feldspars, and almandine making spherical structures easily visible. Spherical grains were then manually

separated from the bulk sample and the remaining bulk magnetic sample retained for further analysis and the process repeated. Once no more magnetic spherules were obtained, DI water was added to the original sample to float and retrieve carbon spherules using a #230 (63um) Sieve. Sieved samples were then transferred to a pyrex petri dish and additional DI water was added to separate carbon spherules from silicates. Carbon spherules, figure 18, were collected individually through pipette and remaining water allowed to evaporate.

Numerous spherical magnetic grains were retrieved from the lower pebbly unit and placed into three major classes: black glassy spherules, red glassy spherules, and colorless spherules. Spherules in all classes ranged in shape from spherical to sub spherical to teardrop in nature, rarely exceeded 200um in diameter, and represent a minor portion of the bulk sample.

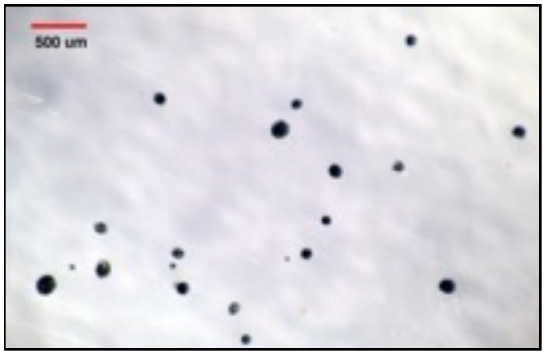


Figure 18: Photomicrograph of representative carbon spherules recovered from grey pebbly loess.

Along with the microspherules numerous scoria-like objects (SLO's) were recovered from the magnetic sample, figure 17. Most SLO's consist of small shards ( < 100um) with some rare vesicular structures as seen in figure 17. SLO's were also subsampled and retained for spectroscopic analysis. Only two carbon spherules were collected from this unit.

Unlike the lower pebbly sand unit, the gray pebbly loess directly above it contains very few SLOs or glassy magnetic spherules. This unit does, however, contain abundant carbon spherules. In total, 182 carbon spherules were recovered from 17.3 grams of sample and range in size from 63um to ~400um with a majority of particles in the 63-100 um range.

Representative examples of all microspherules and SLO's were then prepared for RAMAN spectroscopy by mounting on glass slides prepared with double sided tape. A mounted RockHound portable RAMAN was then used to obtain unoriented RAMAN spectra of individual

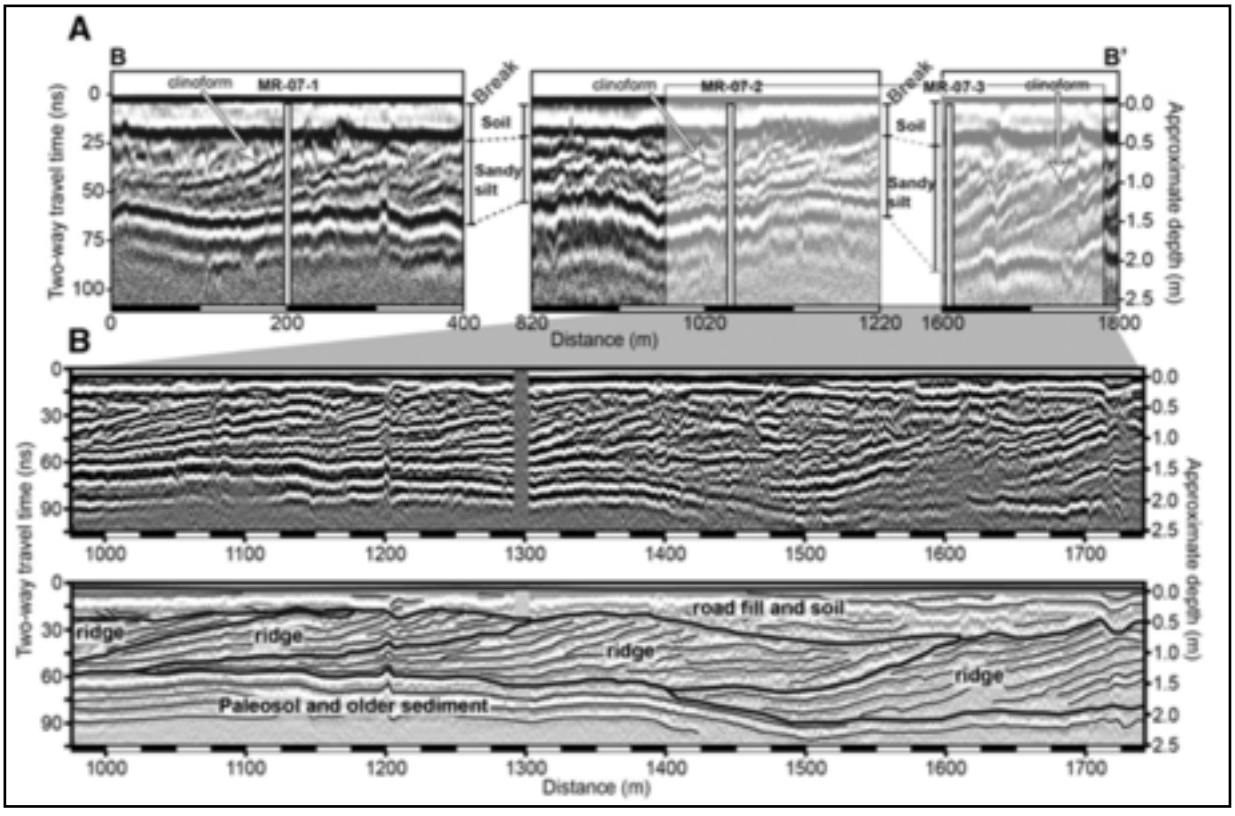


Figure 19: GPR transect across inner ridge of Lake Mattamuskeet showing crossbedded units overlaying older sediments. Adapted from (Rodriguez 2012)

specimens for comparison between known mineral spectra and comparative specimens within the sample.

It should be noted that RAMAN spectroscopy can not be used to determine the source of microspherules or SLO's and its use in this study is simply for compositional comparison. Specifically, spectra of suspected microspherules will be compared to that of magnetite, hematite, almandine, and quartz to distinguish between well weathered glacially transported material and glassy microspherules—all specimens will also be automatically compared to 20,000 other known mineral spectra, see appendix 2.

**Discussion**

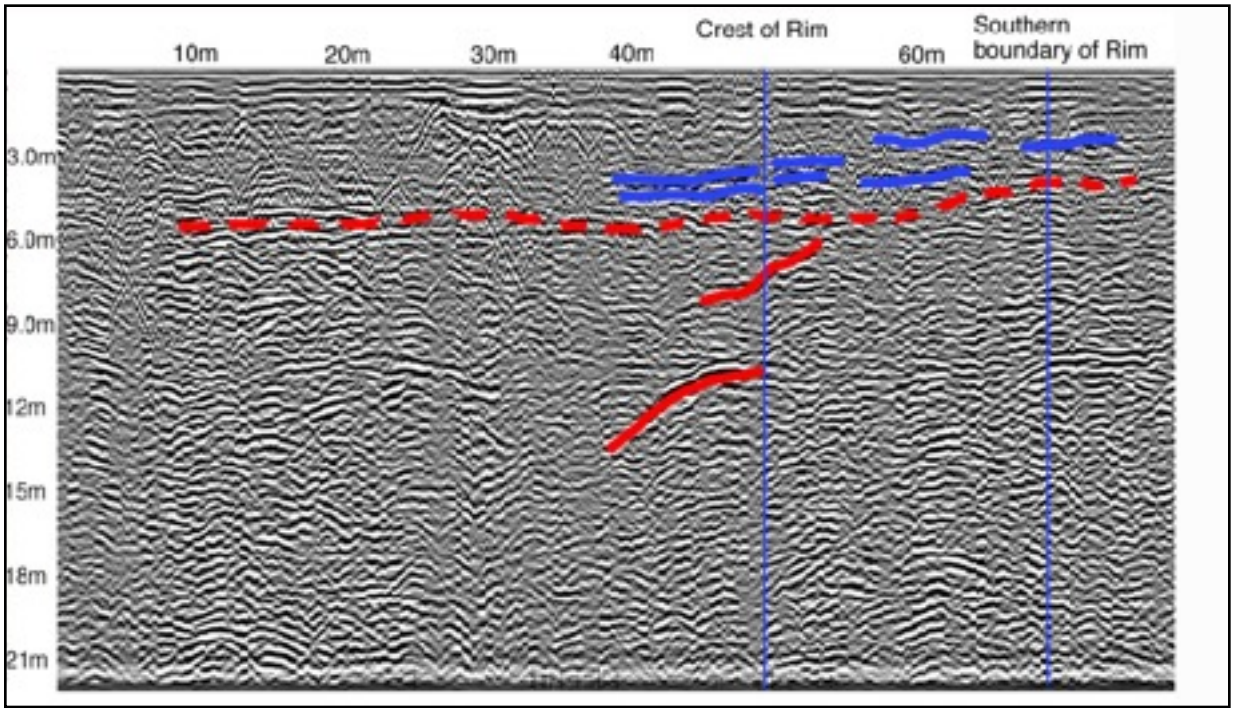


Figure 20. 200mHz Radargram showing first 90 meters of N-S GPR track. Vertical blue lines indicating the position of the rim along site 1.

Very little work has been done to provide concrete results on the formation of Carolina bays. As stated previously numerous processes, such as impacts and aeolian processes, have been suggested for the development of these depressions. Work by Rodriguez (2012) and Grant (1998) suggest that bay rims were not the result of one single event but multiple post Younger Dryas accretionary events (Rodriguez, 2012). This hypothesis relies on the earlier formation of a depression which is then episodically occupied by a lake providing near-shore lake deposits which act as the source for subsequent dune creation forming the rim of the bays (Rodriguez, 2012).

As seen in figure 19, GPR transects across the parabolic ridge forming the eastern rim of Lake Mattamuskeet shows distinctive crossbedded units that support the theory that this bay formed through a combination of lake shore and dune development.

Results of the N-S GPR transect in this study do not appear to agree with the proposed mechanism of rim development put forth by Rodriguez, Brooks, and Grant. Although there is a clear distinction between the upper and lower units, parallel bedding within the upper unit suggests it was deposited after initial formation of the depression.

As can be seen in figure 20, only two reflectors (shown in red) correlate well with the location of the rim. However, these reflectors seem to terminate at the boundary between the upper and lower units, shown by the dashed red line. Beds within the upper unit, shown in blue, do not appear to have been deformed and therefore must have been deposited after the event that led to the initial deformation of the lower unit. Although formation of a depression prior to formation of the rim does initially agree with previous findings, unlike previous studies there is no evidence of aeolian processes/crossbedding within the upper unit that would indicate dune formation. Alternatively, although auger sampling was unable to proceed deeper than 1.8 meters, initial sampling seems to indicate a fining upward sequence that may be the result of graded bedding form from ejecta immediately following an impact cratering event. This hypothesis would need to be confirmed through additional sampling to confirm the extent and existence of graded beds within the regions surrounding the bay-like structures, along with high frequency GPR to better resolve bedding within the upper unit.

Further collaborating an impact related mechanism for the formation of Long Island's bay-like structures is the presence of microspherules and scoria-like objects within the upper unit of the depression. As noted by van Hoesel (2014), microspherules can be produced through other means, such as meteoric ablation and "various sedimentary, diagenetic, and artificial processes" (Van Hoesel 2014); however, initial spectroscopic results show that recovered microspherules do not appear to be the results of sedimentary or diagenetic processes as the spectra did not match that of any known mineral; with the exception of the large clear spherule that showed the characteristic peak for almandine at 910 $cm^{-1}$ as well as the 1350 $cm^{-1}$ peak seen in the SLO's. As can be seen in appendix 2 the closest spectral matches occurred between microspherules and the scoria-like objects suggesting similar compositional (glass-like) structure. Further analysis is required to determine the exact isotopic composition of recovered microspherules for comparison to known compositional characteristics of cosmic spherules, volcanic spherules, and those produced as a result of local impacts.

SLOs are often dismissed as volcanic debris which is a common component of atmospheric particulates though it only represents a minor fraction, "orders of magnitude smaller than that of loess," within total global averages (Navrátil, 2013). Nonetheless, Navrátil (2003) succeeded in showing the occurrence of volcanic particulates from the 2010 Eyjafjallajökull eruption in dust deposition in Prague, CZ: roughly 2,500 miles from the eruption based on the modeled atmospheric trajectory of the particulates. The majority of particulates collected within that study ranged in size from 1 to 50um with particles reaching 100um in diameter being described as "very rare (Navrátil, 2013)."

There are numerous North American volcanoes within similar distance to Long Island as Prague is to Eyjafjallajökull and weather patterns could potentially bring volcanic particulates to the area. Amboy Crater, Black Butte, the Cima volcanic field, and Mt Konocti all have been reported to have erupted between 11,000-9,500 yr BP (USGS, 2014) but whether particulates from the eruptions, given the size of the eruptions, would reach Long Island at the sizes recovered from the Rocky Point site would be highly debatable. Although SLO's are rare within the Rocky Point site samples, the relative sizes of these particles suggest a source nearer than 2,500 miles

which would exclude all North American volcanoes. Furthermore atmospheric circulation currents would most like preclude any Icelandic or European volcanic particulates of the sizes seen within this study from reaching the region of the study site.

Bunch et al. (2012) concluded that SLO's recovered from North American sites (within similar depths as those described in this study) and in the Middle East were most similar to those produces as a result of nuclear airburst, cosmic airbursts, and impact crater plumes based on their similar composition to local sediments (Bunch, 2012). Bunch (2012) also noted that formation of SLOs required temperatures in excess of 2,200°C to melt the local sediment. However, any impact capable of producing temperatures within this range would also produce craters much larger than the suspected craters found on Long Island (Collins, 2005). This suggest that SLOs found within the Rocky Point site were not produced locally and if the Long Islands bay-like features are impact-related they are the result of secondary impactors from a larger distant impact.

Dramatic increases in the abundance of carbon microspherules have also been cited in numerous studies as a major marker of the YD impact event and, as described earlier, similar findings have been made at the Rock Point study site. Firestone et al. (2007) suggest the presence of nanodiamonds and fullerenes (some of which contain $He^3$) found within some carbon spherules can only be explained through extra terrestrial impact while the carbon spherules themselves were the result of forest fires ignited by thermal radiation from the impact event (Firestone, 2007). However Van Hoesel (2004) points out that nanodiamonds are routinely produced through meteoric ablation and should be present, to some degree, continuously in the sediment profile. Van Hoesel further states that meteoric rain could not account for the presence of nano diamonds within carbon spherules (van Hoesel, 2014) and although nano diamonds and He3 remains a controversial aspect of the Younger Dryas impact theory the presence of a peak abundance of carbon microspherules along the Allerod-YD boundary is consistent among study sites.

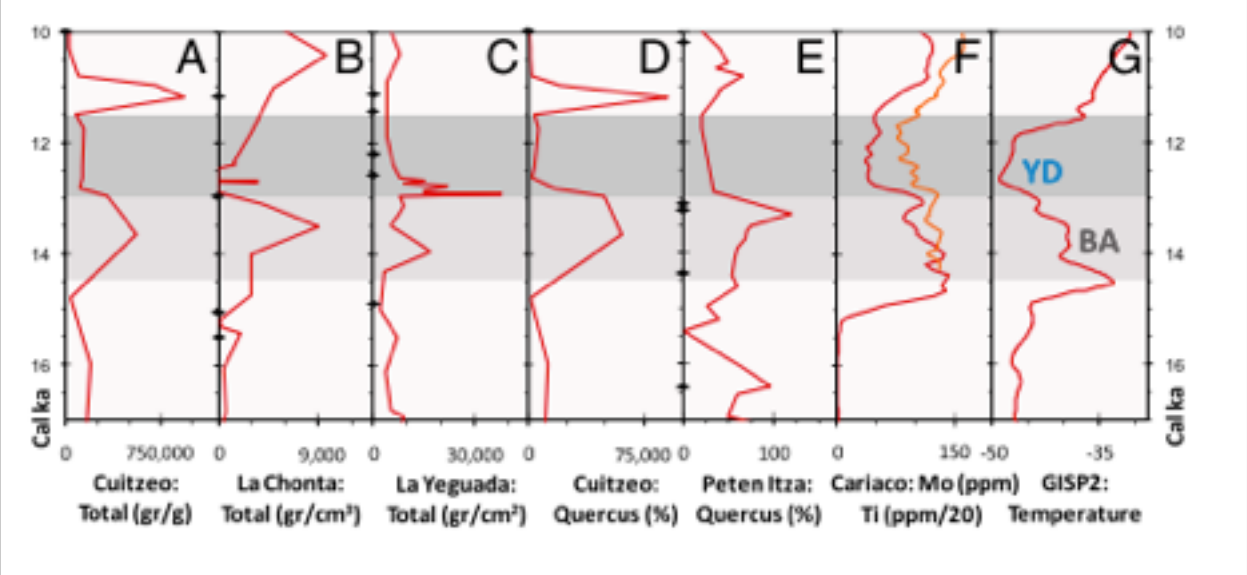


Figure 22: Chart showing pollen abundance at Central Mexican Allerod-YD boundary sites. Adapted from Israde, 2012.

Along with the dramatic increase of carbon microspherules, Israde et al. (2012) also showed a similarly dramatic decrease in both pollen diversity and abundance, see figure 22 (Israde, 2012). This decrease in pollen abundance has typically been associated with a decrease in biodiversity as a result of the impact and subsequent cooling during the younger dryas. However, as seen in figure 22, some of the decreases in pollen abundance begin prior to the A-YD boundary and continue across the boundary and therefore may be indicative of ecological change in response to rapid climate change and not necessarily indicative of the cause.

Furthermore, Scott (2010) notes that although carbon microspherules do not appear to contain evidence of seed-like morphologies or plant-like cellular structure as originally described by Firestone (2007) they do appear to have similar morphologies to fungal sclerotia. Although the original surface of fungal sclerotia may contain ridges and troughs, as noted by Scott, under only moderate heating, at a temperature of 350°C, the surface becomes smooth and glassy and transitions from brown to black with external and internal structures very similar to those reported for collected carbon microspheres (Scott, 2010). Although typically considered a very resilient material pollen has also been carbonized at relatively low temperatures (300°C—600°C) for the industrial preparation of micro spherical support structures (Wang, 2005). As shown by Bailey (1980) these temperatures are consistent with soil temperatures within forest, grassland, and scrubland fires and therefore the presence of carbon microspherules may simply represent charring of previously deposited materials. Van Hoesel also points out that nanodiamonds combust at temperatures above 600°C therefore a peak abundance of nano diamonds, if confirmed, in YD boundary sediments would further constrain local temperatures during the event that led to their formation (van Hoesel, 2014). It is therefore possible that decreases in pollen and increases in carbon microspherules are directly related with one being the result of charing the other.

**Conclusion**

Despite the stratigraphic and geophysical data described in this study the formation of Long Island's bay-like structures, specifically those located in the Rocky Point Resource Management Area, remain a mystery. Although initial findings do not definitively rule out any of the proposed mechanisms of formation of Carolina bay-like structures the occurrence of scoria-like objects and microspherules are a provocative finding that lends credence to an impact-related event. Although carbon microspherules themselves may be produced through local natural fires, the prevalence of these materials over a short interval of similar age across North America and the Middle East has yet to be definitively explained.

Further studies of the sites included in this paper with high frequency gpr are required to elicit more resolved detail of near surface stratigraphical features for comparison to other published accounts of similar features. Also a more complete quantitative study of the abundance of microspherules and SLO's across the boundary identified within this study is required for comparison to background levels and vertical mapping of pollen and microspherule abundances for correlation to similar features within the region.

Appendix 1

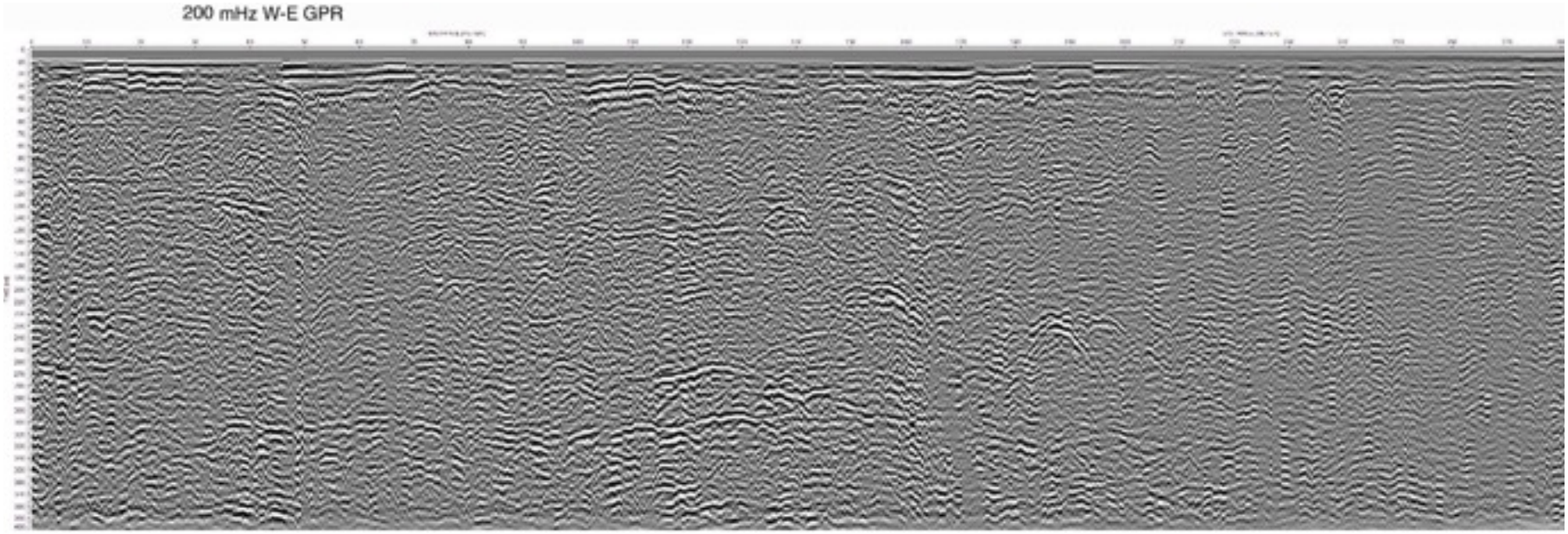


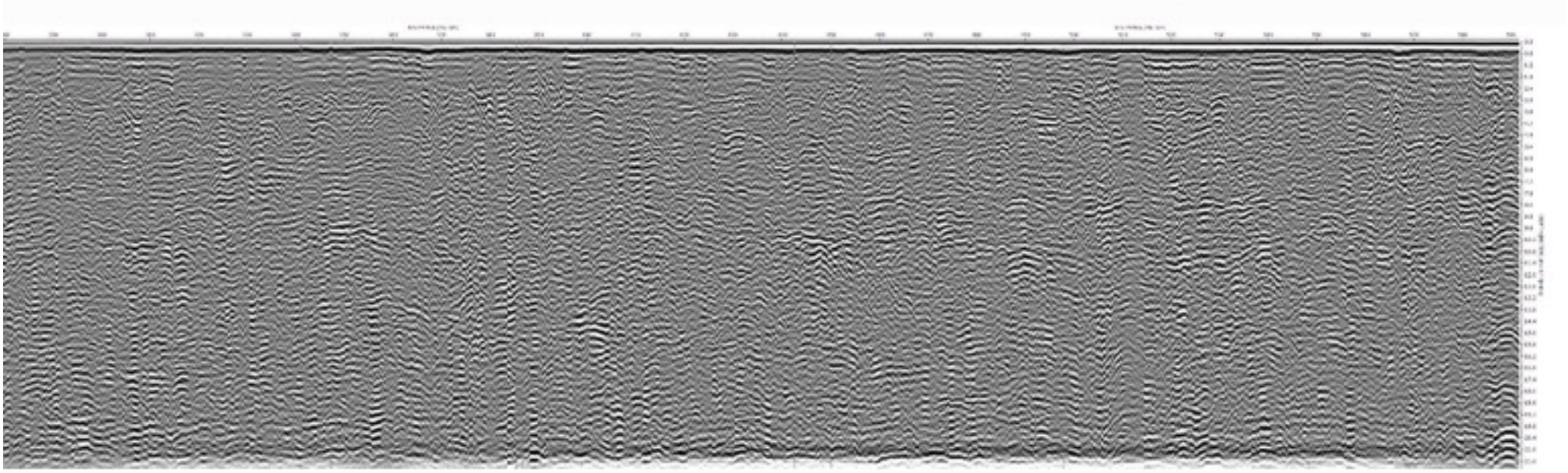

Appendix 2

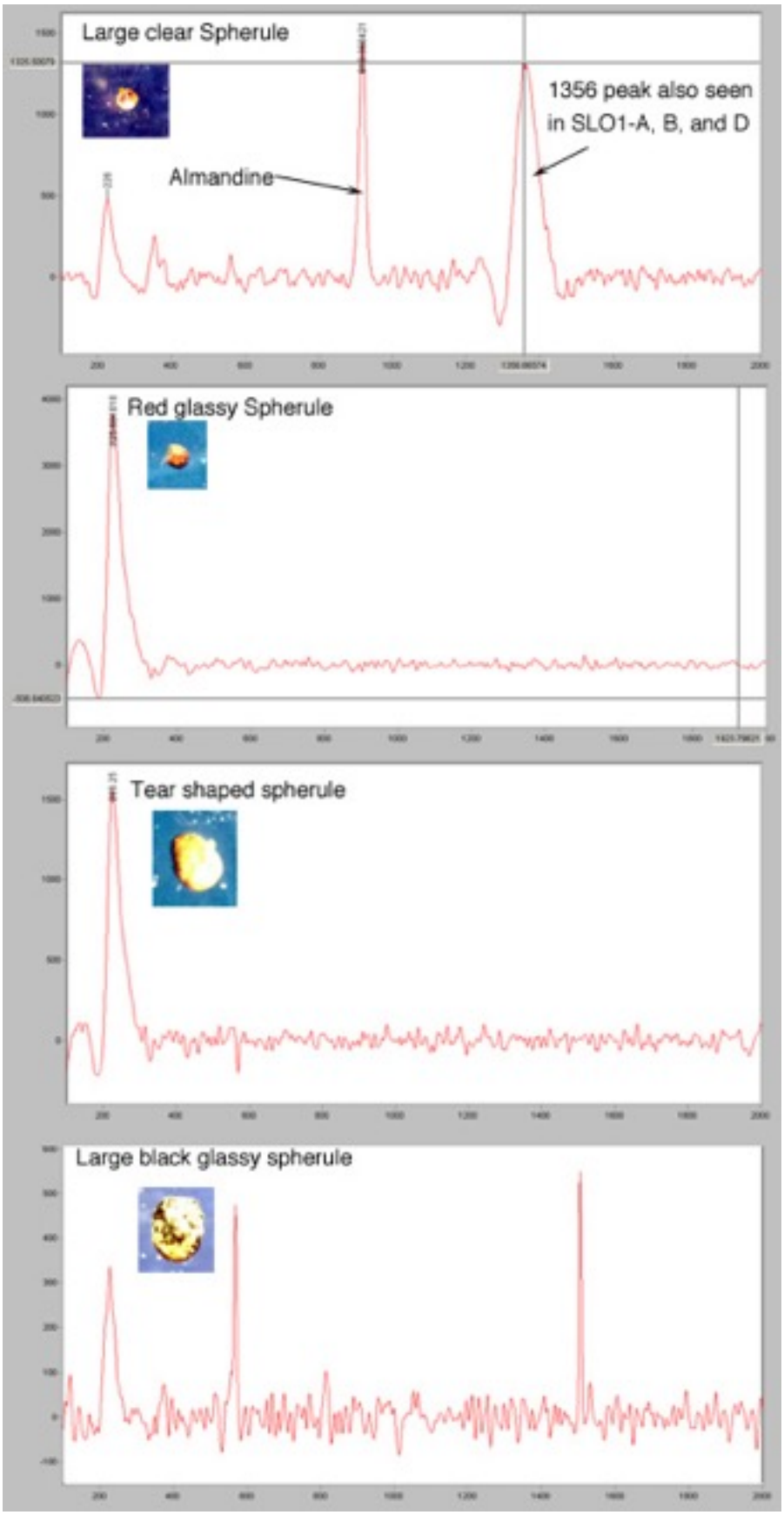
Large clear Spherule
1356 peak also seen in SLO1-A, B, and D
Almandine
Red glassy Spherule
Tear shaped spherule
Large black glassy spherule

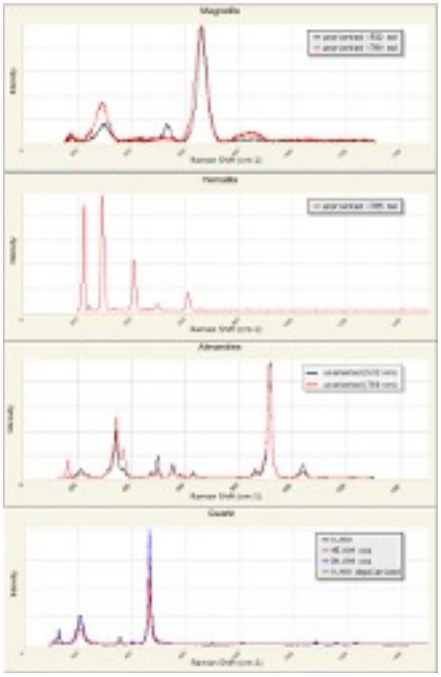

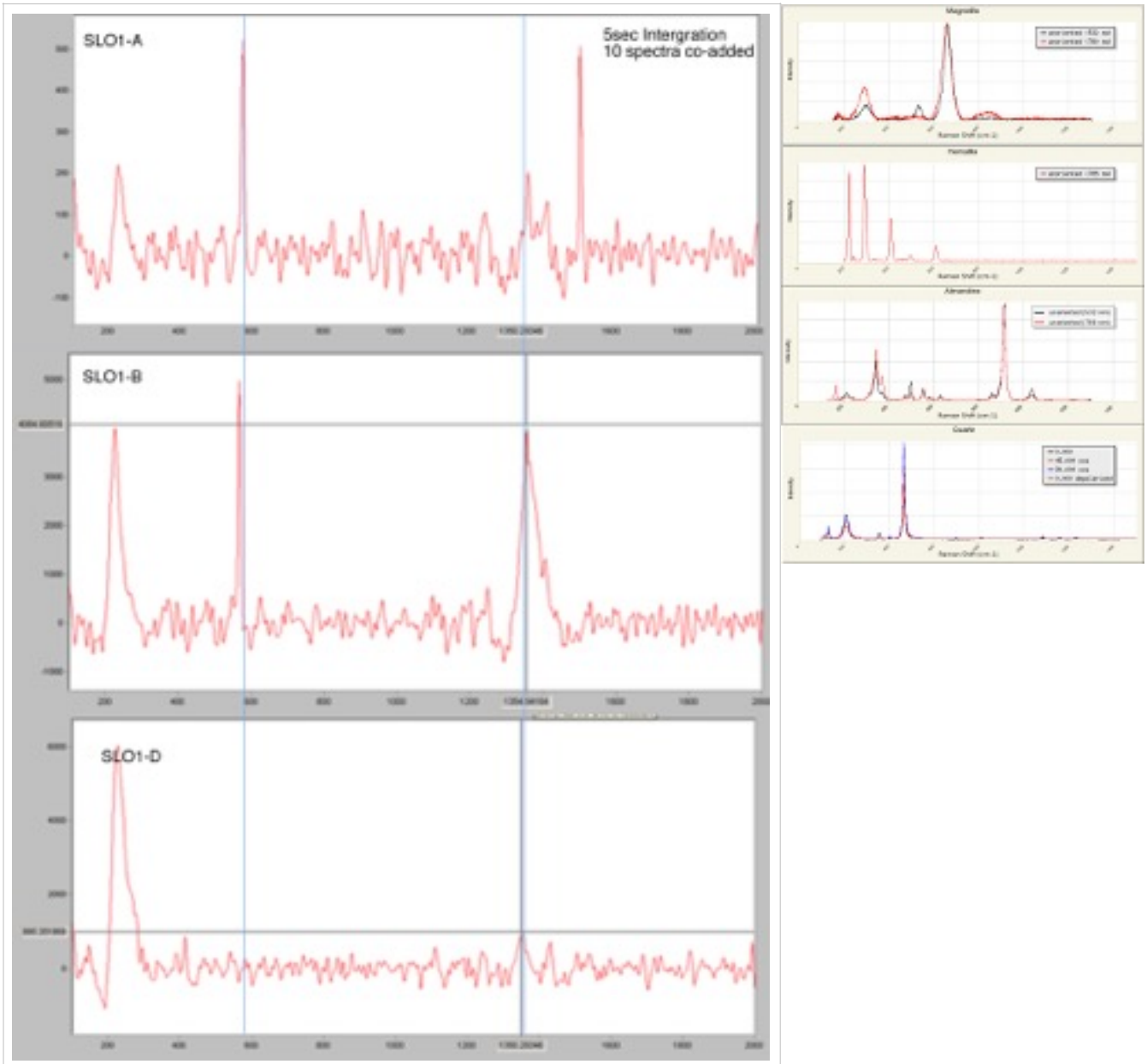


Figure 18: RAMAN Spectra of scoria-like objects A, B, and D.

**Bibliography**


*Advance_Identification-of-CarolinaBays.pdf.* (n.d.).. S.C Department of Natural Resources. Retrieved from http://www.dnr.sc.gov/wildlife/docs/CarolinaBays.pdf

Baales, M., Jöris, O., Street, M., Bittmann, F., Weninger, B., & Wiethold, J. (2002). Impact of the late glacial eruption of the laacher see volcano, central rhineland, germany. *Quaternary Research*, *58*(3), 273-288. doi:10.1006/qres.2002.237

Bailey, A. W., & Anderson, M. L. (1980). Fire temperatures in grass, shrub and aspen forest communities of central alberta. *Journal of Range Management Archives*, *33*(1), 37-40.

Bunch, T. E., Hermes, R. E., Moore, A. M., Kennett, D. J., Weaver, J. C., Wittke, J. H., . . . Howard, G. A. (2012). Very high-temperature impact melt products as evidence for cosmic airbursts and impacts 12,900 years ago. *Proceedings of the National Academy of Sciences*, *109*(28), E1903-E1912.

Collins, G. S., Melosh, H. J., & Marcus, R. A. (2005). Earth impact effects program: A web-based computer program for calculating the regional environmental consequences of a meteoroid impact on earth. *Meteoritics & Planetary Science*, *40*(6), 817-840. doi:10.1111/j.1945-5100.2005.tb00157.

de Klerk, P., Janke, W., Kühn, P., & Theuerkauf, M. (2008). Environmental impact of the laacher see eruption at a large distance from the volcano: Integrated palaeoecological studies from vorpommern (NE germany). *Palaeogeography, Palaeoclimatology, Palaeoecology*, *270*(1-2), 196-214. doi:10.1016/j.palaeo.2008.09.01

Firestone, R. B., West, A., Kennett, J. P., Becker, L., Bunch, T. E., Revay, Z. S., . . . Erlandson, J. M. (2007). Evidence for an extraterrestrial impact 12,900 years ago that contributed to the megafaunal extinctions and the younger dryas cooling. *Proceedings of the National Academy of Sciences*, *104*(41), 16016-16021.

Gill, G. (n.d.). *Documenting the occurrence of carolina bays on long island*.

Grant, J. A., Brooks, M. J., & Taylor, B. E. (1998). New constraints on the evolution of carolina bays from ground-penetrating radar. *Geomorphology*, *22*(3), 325-345.

Holliday, V. T., Surovell, T., Meltzer, D. J., Grayson, D. K., & Boslough, M. (2014). The younger dryas impact hypothesis: A cosmic catastrophe. *Journal of Quaternary Science*, *29*(6), 515-530. doi:10.1002/jqs.272

Rodriguez, A. B., Waters, M. N., & Piehler, M. F. (2012). Burning peat and reworking loess contribute to the formation and evolution of a large carolina-bay basin. *Quaternary Research*, *77*(1), 171-181. doi:10.1016/j.yqres.2011.11.004

Michikami, T., Hagermann, A., Miyamoto, H., Miura, S., Haruyama, J., & Lykawka, P. S. (2014). Impact cratering experiments in brittle targets with variable thickness: Implications for deep pit craters on mars. *Planetary and Space Science*, *96*, 71-80.

Navrátil, T., Hladil, J., Strnad, L., Koptíková, L., & Skála, R. (2013). Volcanic ash particulate matter from the 2010 eyjafjallajökull eruption in dust deposition at prague, central europe. *Aeolian Research*, *9*, 191-202. doi:10.1016/j.aeolia.2012.12.00

Pinter, N., Scott, A. C., Daulton, T. L., Podoll, A., Koeberl, C., Anderson, R. S., & Ishman, S. E. (2011). The younger dryas impact hypothesis: A requiem. *Earth-Science Reviews*, *106*(3-4), 247-264. doi:10.1016/j.earscirev.2011.02.00

van Hoesel, A., Hoek, W. Z., Braadbaart, F., van der Plicht, J., Pennock, G. M., & Drury, M. R. (2012). Nanodiamonds and wildfire evidence in the usselo horizon postdate the allerød-younger dryas boundary. *Proceedings of the National Academy of Sciences*, *109*(20), 7648-7653

van Hoesel, A., Hoek, W. Z., Pennock, G. M., & Drury, M. R. (2014). The younger dryas impact hypothesis: A critical review. *Quaternary Science Reviews*, *83*, 95-114. doi:10.1016/j.quascirev. 2013.10.033

Wang, X., Luo, L., Guo, H., Mu, L., Li, C., Ji, W., & Cai, H. (2013). Cratering process and morphological features of the xiuyan impact crater in northeast china. *Science China Earth Sciences*, *56*(10), 1629-1638. doi:10.1007/s11430-013-4695-

USGS. 2014. Volcanic Hazards Program. URL http://volcanoes.usgs.gov/volcanoes/clear_lake/